Proc. Natl. Acad. Sci. USA
Vol. 92, pp. 12131–12135, December 1995
Biochemistry

Interaction between the phage HK022 Nun protein and the *nut* RNA of phage λ

(RNA–protein interaction/transcription termination)

SAMIT CHATTOPADHYAY*†, SIU CHUN HUNG†‡§, ASHLEY C. STUART†‡, ARTHUR G. PALMER III‡, JAIME GARCIA-MENA*, ASIS DAS*, AND MAX E. GOTTESMAN‡§

*Department of Microbiology, University of Connecticut Health Center, Farmington, CT 06030; and ‡Department of Biochemistry and Molecular Biophysics and §Institute of Cancer Research, Columbia University College of Physicians and Surgeons, New York, NY 10032

Communicated by F. William Studier, Brookhaven National Laboratory, Upton, NY, August 11, 1995

ABSTRACT **The *nun* gene product of prophage HK022 excludes phage λ infection by blocking the expression of genes downstream from the λ *nut* sequence. The Nun protein functions both by competing with λ N transcription-antitermination protein and by actively inducing transcription termination on the λ chromosome. We demonstrate that Nun binds directly to a stem–loop structure within *nut* RNA, *boxB*, which is also the target for the N antiterminator. The two proteins show comparable affinities for *boxB* and they compete with each other. Their interactions with *boxB* are similar, as shown by RNase protection experiments, NMR spectroscopy, and analysis of *boxB* mutants. Each protein binds the 5′ strand of the *boxB* stem and the adjacent loop. The stem does not melt upon the binding of Nun or N, as the 3′ strand remains sensitive to a double-strand-specific RNase. The binding of RNA partially protects Nun from proteolysis and changes its NMR spectra. Evidently, although Nun and N bind to the same surface of *boxB* RNA, their respective complexes interact differently with RNA polymerase, inducing transcription termination or antitermination, respectively.**

Gene expression in phage λ and other lambdoid phages is temporally regulated by a mechanism of transcription termination and antitermination (1–5). The expression of the early λ operons requires the suppression of transcription termination signals by a sequence-specific RNA-binding protein, the 107-aa product of the λ *N* gene. The N protein stabilizes transcription elongation by interacting with λ *nut* RNA and RNA polymerase (RNAP) in association with host Nus factors (2–9). The λ *nut* site is divisible into two parts, *boxA* and *boxB*. The *boxA* sequence is 10 nt long, and *boxB* is a 15-nt stem–loop structure. The *boxA* sequence lies a few nucleotides upstream of *boxB*. NusB and NusE (S10) specifically interact with *boxA* (10). The N protein specifically interacts with the loop sequence and one face of the stem sequence of *boxB* (11).

The *nun* product of coliphage HK022 is a 109-aa protein that excludes superinfecting λ by provoking transcription termination at or just distal to the λ *nut* sites (12–15). Nun termination mimics N antitermination in its requirements for cis-acting sites and host factors, both reactions requiring the λ *nut* site and the host Nus proteins for optimal efficiency (16). Mutations in *nut* inhibit both N and Nun (12, 17). Certain *nusA*, *nusB*, and *nusE* mutations inhibit both functions (12); however, some *nusA* mutations and mutations in *nusG* and in *rpoC* (encoding the β′ subunit of RNAP) are Nun-specific (18). Exclusion of λ by HK022 prophage is suppressed by overproduction of N (12). Competition between Nun and N has been demonstrated in a minimal *in vitro* transcription system that includes a λ *nut* DNA template and RNAP (15). In addition, *boxB* RNA added in excess inhibits Nun transcription-arrest activity *in vitro* (15).

In this paper we demonstrate that Nun specifically binds *boxB* RNA. The *boxB*–Nun complex was analyzed by gel retardation, RNase footprinting, protease protection, and NMR spectroscopy. We find that Nun and N have overlapping recognition sites. The two proteins compete for binding to *boxB*, which may account for the suppression of Nun function by N *in vivo*.

MATERIALS AND METHODS

RNAs for band-shift and RNase protection experiments were synthesized as described (11). The wild-type λ *nutRboxB* RNA was 5′-GGGCGAAUUGGGUACCGGGCCCCCCCUCGA-**GCCCUGAAAAAGGGC**AUCGAAUU-3′ (*boxB* in bold type) and the P21 stem–λ loop hybrid *boxB* RNA was 5′-GGGCG-AAUUGGGUACCGGGCCCCCCCUCGAGACU**CUCAA-CGAAAAGUUGAG**AAUU-3′ (hybrid *boxB* in bold type). RNA oligonucleotides used in NMR and protease assays (λ *nutLboxB* 16-mer; 5′-GGCCCUGAAGAAGGGC-3′; mutant 16-mer: 5′-GGCCCUAAAGAAGGGC-3′) were synthesized by T7 RNA polymerase using synthetic oligodeoxyribonucleotide templates (19). None of the RNAs contain *boxA*. The DNA templates were 5′-AGAAATTAATACGACTCAC-TATA-3′ and 3′-TCTTTAATTATGCTGAGTGATAT**CCGG-GAYTTCTTCCCG**-5′ (*boxB* in bold type).

Transcription was performed with 4 mM NTPs to minimize abortive transcription products. Full-length RNA was purified by electrophoresis in 20% polyacrylamide/8 M urea gels and electroeluted (Schleicher & Schuell) into Tris/borate/EDTA buffer (pH 8.0). RNA was washed in 50 mM sodium phosphate buffer (pH 5.5) with 1 M NaCl and exchanged into 50 mM sodium phosphate buffer (pH 5.5) with a Centriprep-3 (Amicon). RNA was ethanol precipitated and dissolved in the appropriate buffer for further assays. Prior to use, RNA samples were heated to 90°C and rapidly cooled in an ice bath to prevent oligomerization.

For experiments other than the NMR analysis, Nun was purified as described (15). To obtain the higher yield of Nun required for the NMR studies, *nun* was subcloned into another overproducing plasmid, pET21D (Novagen), and expressed in *Escherichia coli* BL21(DE3)/pLysS. Nun protein was purified by ion-exchange column chromatography using SP-Sepharose fast flow and Mono-S resins (Pharmacia). The purified protein migrated as a single band by SDS/PAGE. Nun was dialyzed into the appropriate buffer for NMR spectroscopy or trypsin digestion and concentrated with a Centricon-10 (Amicon).

For band-shift experiments, typical reaction mixtures (20 μl) contained fixed amounts of a 53-nt ^{32}P-labeled RNA (10 nM) that included λ *nutRboxB* (but not *boxA*) as well as vector

The publication costs of this article were defrayed in part by page charge payment. This article must therefore be hereby marked "*advertisement*" in accordance with 18 U.S.C. §1734 solely to indicate this fact.

Abbreviations: RNAP, RNA polymerase; ARM, arginine-rich motif.
†S.C., S.C.H., and A.S. contributed equally to this work.

sequences (11). To this RNA was added various amounts of either N or Nun protein (0–350 nM), 20 mM Tris acetate (pH 7.9), 2 mM magnesium acetate, 60 mM potassium acetate, 1 mM dithiothreitol, 5% (vol/vol) glycerol, and poly(A)·poly(U) (Sigma) at 0.1 mg/ml as nonspecific competitor. After incubation at 0°C for 5 min, 10-μl samples were directly loaded without marker dye onto a nondenaturing 5% polyacrylamide gel and electrophoresed at 4°C for 4 hr at 150 V. Electrophoresis was monitored with a control sample containing bromophenol blue. RNA bands were quantified with a Betascope 603 blot analyzer (Betagen, Waltham, MA); the gels were then dried and autoradiographed.

RNase protection experiments were performed as described (11).

Protection of Nun from trypsin proteolysis upon complex formation was tested by digesting Nun in the absence or presence of RNA. In all samples, the Nun concentration was 20 μM in 50 mM sodium phosphate (pH 5.5). Samples contained equimolar amounts of *boxB* RNA 16-mer (sufficient to yield a 1:1 complex with Nun), equimolar amounts of mutant 16-mer, or no RNA. Trypsin (Sigma) was added (1:250, wt/wt) and incubated for 1 hr at 37C. Samples were analyzed by SDS/16% PAGE.

NMR data were collected on a Bruker (Billerica, MA) model AMX500 spectrometer at 280 K. Proton spectra were recorded with a jump–return pulse sequence to minimize saturation transfer from water to exchangeable protons. Spectra were recorded with 256 transients. All data were processed with FELIX 2.10 (Biosym Technologies, San Diego). The NMR sample initially contained 0.5 mM *boxB* RNA 16-mer in 10 mM potassium phosphate buffer/100 mM KCl/0.02% sodium azide, pH 7.0, in $^1H_2O/^2H_2O$ (9:1, vol/vol). Nun protein was titrated into the RNA in 15-μl aliquots of 1.5 mM Nun in the same buffer. NMR spectra were collected after each addition of the Nun protein and corrected for dilution. After each Nun addition during the titration, 2-μl aliquots of the Nun–*boxB* RNA complex were removed and were analyzed by electrophoresis in a nondenaturing 7.5% polyacrylamide gel at 4°C. Gels were stained consecutively with ethidium bromide and Coomassie blue R-250.

RESULTS

Nun Binds to the *boxB* RNA Hairpin. A 53-nt ^{32}P-labeled RNA substrate that includes the *boxB* RNA hairpin was incubated with various amounts of purified Nun protein (Fig. 1*A*). This RNA is homogeneous by denaturing gel electrophoresis. On nondenaturing gels, we observe multiple bands, likely representing various conformers of the RNA monomer and a dimer, that arise due to the self-complementarity of the vector-derived sequence of the RNA (11). Upon binding, both N and Nun form several nucleoprotein complexes (Fig. 1*A*). Based on studies of N–*boxB* complexes, we believe that the complexes marked C1 and C2 are produced from the monomeric RNA species and that C3 and C4 are complexes of Nun with dimeric RNAs. At low concentrations of Nun, only one promoter binds to the dimeric RNA, yielding complex C3. At higher Nun concentrations both hairpins in the RNA dimer are occupied, forming C4. The pattern of Nun complexes suggests that a protein monomer interacts with one RNA hairpin. As with N, no host factor is required for the interaction of Nun with RNA. The conditions used for Nun binding to RNA differ somewhat from those described for N; Nun binding to *boxB* is inhibited by high (>5 mM) Mg^{2+} ion concentrations (data not shown). In acetate buffer, the estimated K_d of the Nun–*boxB* complex is 47.5 nM, about twice that of N (Fig. 1*B*). Although the two proteins are of nearly same size, the Nun–*boxB* complexes migrate more slowly than the N–*boxB* complexes (Fig. 1*A*). This may be due to the higher positive charge of Nun, or a structural difference between the two complexes.

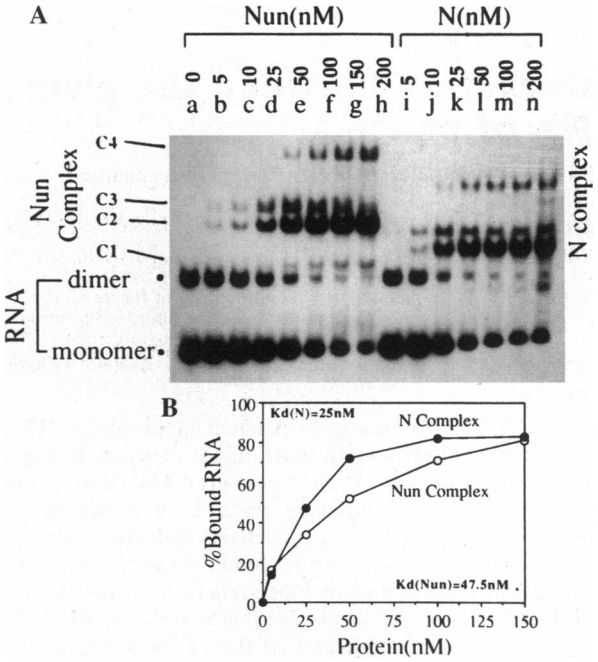

FIG. 1. Interaction of N and Nun proteins with *boxB* RNA. (*A*) A 53-nt RNA (10 nM) containing the λ *nutRboxB* sequence (11) was tested for binding by a gel retardation assay. Free RNA (lane a) appears as monomers and dimers. Complexes formed by Nun (*Left*) are marked (C1–C4). Complexes formed by N protein are also shown (*Right*). The concentrations of N and Nun are shown at the top. (*B*) K_d values were calculated from the bound and unbound RNA present in each nucleoprotein complex.

Mutational Analysis of *boxB*. To analyze interactions between Nun and the *boxB* loop (GAAAA), we measured Nun binding after replacing each base in the single-stranded loop with the other three bases (11). A fixed amount of labeled *boxB* RNA (10 nM) was incubated with a 10-fold excess of Nun protein (100 nM), and the samples were run on a nondenaturing gel to separate nucleoprotein complexes from free RNA (Fig. 2). All of the base replacements in the first position abolished Nun binding. This base was also critical for the transcription-arrest activity of Nun (15). Substitutions in position 5 also reduced Nun binding, but less dramatically. Position 4 substitutions, including the A-to-G substitution that distinguishes *nutR* from *nutL*, did not affect Nun binding. Pyrim-

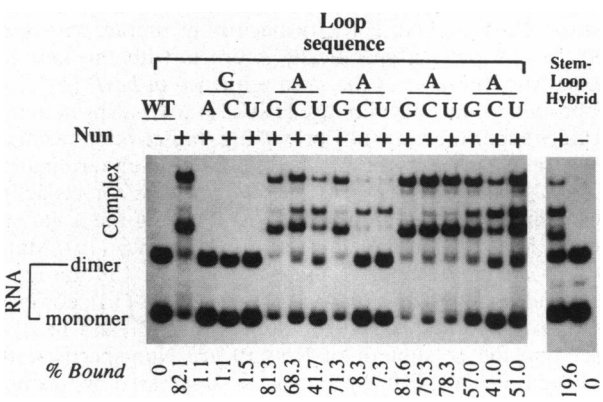

FIG. 2. Effects of base replacement in *boxB* stem and loop. The binding of Nun protein to the wild type λ *boxB* (WT) and various λ-*boxB* loop mutant RNAs (10 nM) was examined in the presence of 100 nM purified protein. Both free RNA and bound RNA complexes are marked at left. Hybrid *boxB* RNA (phage P21 stem and λ loop) is shown in the two rightmost lanes in the presence or absence of Nun protein. The amount of complex (C1 + C2 + C3) formed is indicated below the gel.

idine substitutions in the second and third positions reduced Nun binding to various extents, whereas A-to-G changes in those positions showed only weak effects. Taken together, these results indicate that position 1 is the most critical for Nun binding and may, therefore, participate in specific base–amino acid contacts. With the exception of the fourth base, the other loop residues are also involved in Nun recognition, either through contacts with Nun or by specifying the configuration of the *boxB* RNA. The effects of *boxB* loop mutations on the binding of N and Nun are summarized in Table 1.

To determine whether the sequence of the *boxB* stem also affected Nun binding, we replaced the λ stem with the heterologous *boxB* stem of the Nun-resistant phage P21 (see *Materials and Methods*). The hybrid RNA formed nucleoprotein complexes with Nun protein with similar migration patterns as the λ *boxB* complexes. However, the binding affinity of Nun with this hybrid RNA sequence was reduced significantly relative to the λ *boxB* stem (20% vs. 80% of RNA bound at 100 nM Nun) and was comparable to some of the highly defective loop mutants (Fig. 2, two rightmost lanes). These data suggest that Nun interacts both with the *boxB* loop and with the *boxB* stem region.

Nun Binds to a Subdomain of *boxB* RNA. We performed RNase footprinting assays to determine the points of contact between Nun protein and the *boxB* RNA hairpin and to detect potential changes in RNA structure. For these experiments, we used a 96-nt end-labeled RNA derived from λ *nutR* containing both *boxA* and *boxB* sequences and three RNases with different specificities. RNases T1 and T2 cleave between unpaired RNA bases, whereas RNase VI cleaves duplex RNA. RNase T1 cleaves 3′ to G residues; RNase T2 cleaves 3′ to any residue. The cleavage patterns of RNases T1, T2, and VI reflect the hairpin structure of *boxB* (Fig. 3). The four 5′-proximal bases of the loop were accessible to RNase T2, whereas some stem bases were accessible to RNase VI. The pattern of RNase digestion was distinctly altered by the addition of Nun. Nun protected loop bases 1–4 from RNase T2 cleavage (lanes d–g), and the 5′ arm, but not the 3′ arm, of the stem from RNase VI cleavage (lanes h–k). This result indicates that Nun protein recognizes the loop and the 5′ subdomain of the *boxB* hairpin, and demonstrates, furthermore, that the binding of Nun does not melt the *boxB* stem. The pattern of protection by Nun closely resembles that of N, determined with the same RNA ligand (11).

Probing the Nun–*boxB* RNA Complex. Nun contains 11 arginine and 12 lysine residues. Trypsin readily digests the protein to completion in the absence of *boxB* RNA. The wild type *boxB* 16-mer, but not a mutant 16-mer (loop position 1A), partially protected Nun from digestion (Fig. 4). This protection suggests that a domain of Nun may become more compact (trypsin-resistant) in the presence of its ligand, the wild-type *boxB* RNA. N-terminal sequencing of the excised gel bands indicates that the protected fragments have native N termini. These results agree with NMR spectra of the Nun protein alone that show little evidence of stably folded, compact tertiary structure (data not shown).

Competition for Nun and N Binding to *boxB* RNA. In view of the similar specificities and protection patterns of Nun and

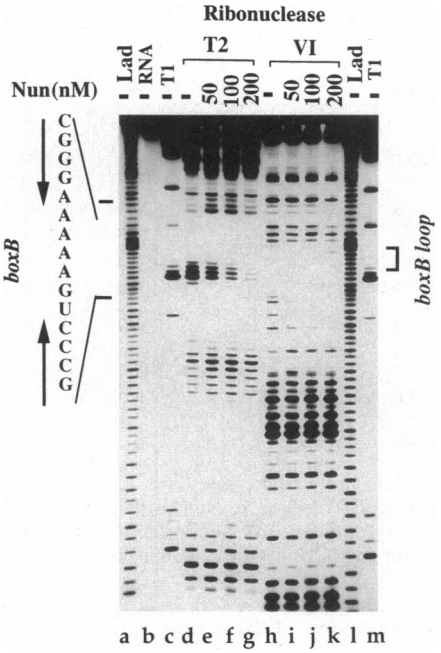

FIG. 3. Identification of Nun–*boxB* contacts by RNase footprinting. A 96-nt end-labeled RNA containing *boxA* and *nutRboxB* was digested with single-strand (T1 and T2)- and double-strand (VI)-specific RNases in the presence or absence of Nun protein. RNA ladders produced by alkaline hydrolysis or RNase T1 digestion of the substrate RNA were used as markers (lanes a, c, l, and m). RNA samples treated with RNases T2 and VI were run in lanes d–g and h–l. Amounts of Nun (nM) used are indicated at the top. The *boxB* region in the RNA is marked. The band that corresponds to the first base of the pentameric loop is shown. Lad, sequence ladder.

N, we thought it likely that the two proteins would compete for binding to *boxB*. To test this, fixed amounts of *boxB* RNA (10 nM) and Nun (100 nM) were incubated with various amounts of N, and the resulting complexes were displayed on nondenaturing gels (Fig. 5 *Left*). As the concentration of N increased, the slow mobility Nun–*boxB* complexes shifted gradually to the fast mobility N-*boxB* complexes (compare lanes a–h from right to left), indicating the displacement of one protein by the other. No evidence of a complex with novel mobility is seen, suggesting that Nun and N did not bind the same RNA molecule simultaneously. Roughly equimolar concentrations of the Nun and N complexes were formed at 25–50 nM N (lanes d and e). Similar competition between the two proteins was observed in a reciprocal experiment in which various amounts of Nun were added to a fixed amount of N and RNA (Fig. 5 *Right*, lanes j–q). With increasing Nun levels, the majority of the N complexes were converted to Nun complexes. Consistent with the N competition result, 50% competition was observed at 2- to 4-fold Nun excess. This is in accord with the estimated dissociation constants for Nun and N complexes with RNA, 47.5 nM and 25 nM, respectively (Fig. 1*B*).

Table 1. Effects of λ *nutRboxB* loop mutations at positions 1–5 on the binding of Nun and N

	Binding				
Base	1	2	3	4	5
G	**+++/+++**	+++/+++	+++/+++	+++/+++	++/+++
A	−/−	**+++/+++**	**+++/+++**	**+++/+++**	**+++/+++**
U	−/−	++/+++	+/+	+++/+++	++/+++
C	−/−	+++/+++	+/+	+++/+++	++/+++

The effects of each loop base substitution on Nun and N binding are indicated as Nun/N: −, +, ++, and +++ indicate increasing affinities of the protein for the *boxB* ligand as shown in Fig. 2 and ref. 11. Bold symbols indicate the wild-type base in that position.

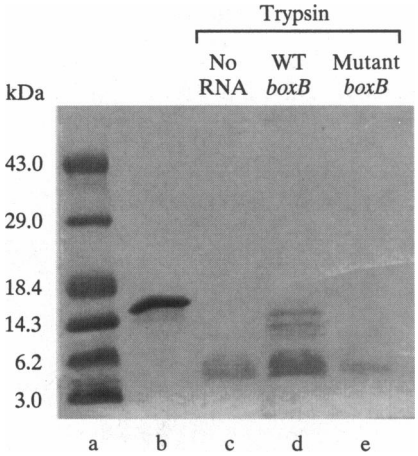

FIG. 4. Trypsin protection assay. Lane a, protein molecular size markers (GIBCO/BRL); lane b, Nun protein; lane c, Nun protein digested with trypsin; lane d, Nun protein with wild-type (WT) *nutLboxB* 16-mer and trypsin; lane e, Nun protein with mutant 16-mer and trypsin.

NMR Spectroscopy of Nun and *boxB* RNA. Interaction between the stem residues of 16-mer *boxB* RNA and Nun was supported by NMR spectroscopy. The Nun tryptophan $H^{\varepsilon 1}$ resonances and the *boxB* 16-mer G and U imino protons are well resolved from other protein and RNA signals and are convenient for monitoring structural changes in the Nun–RNA complex. Imino protons not involved in hydrogen bonding interactions exchange rapidly with bulk solvent H_2O protons, and the NMR resonances are expected to be unobservable. The downfield regions of ^1H NMR spectra of free Nun and *boxB* 16-mer are shown in Fig. 6 (spectra A and B, respectively). The broad resonance at 10.2 ppm arises from Trp-33 and the sharp resonance at 10.1 ppm arises from Trp-109. The five resonances between 12 ppm and 14 ppm in Fig. 6, spectrum B, are indicative of Watson–Crick base-paired G and U nucleotides in *boxB* 16-mer. The NMR spectrum has not been assigned; however, the observed resonances presumably arise from the five base-paired G and U resonances in the *boxB* stem. The resonance at 10.5 ppm in spectrum B may represent a non-Watson–Crick base pair between one of the G–A mismatches in the loop. The midpoint of the thermal melting transition of the hairpin was estimated to be ≈50°C by monitoring the disappearance of the imino peaks as a function of temperature (data not shown). As Nun is added to *boxB* 16-mer, the original imino proton resonances observed in spectrum B gradually disappear, a new set of imino proton resonances appears in the spectra, and the resonance arising from Trp-33 becomes stronger and sharper. The spectrum of the final 1:1 complex between Nun and *boxB* 16-mer is shown in Fig. 6, spectrum C. Nondenaturing gel electrophoresis of aliquots removed from the NMR tube during the titration revealed the gradual disappearance of the free RNA band and the gradual appearance of a shifted RNA band that costained with Coomassie blue (data not shown).

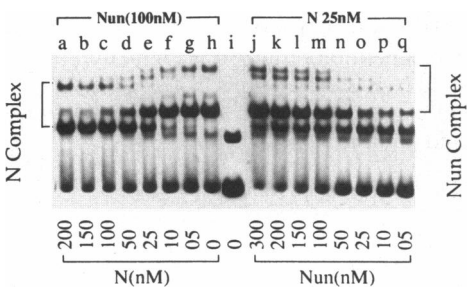

FIG. 5. Competition of Nun and N proteins for *nutRboxB* RNA. *boxB* RNA (10 nM) was run in the absence of protein (lane i). RNA samples were run in the presence of a fixed amount of Nun and decreasing amounts of N (lanes a–h). The same RNA was incubated with a fixed amount of N and decreasing amounts of Nun (lanes j–q). Both N and Nun complexes are shown. The amount of each protein is indicated at the bottom.

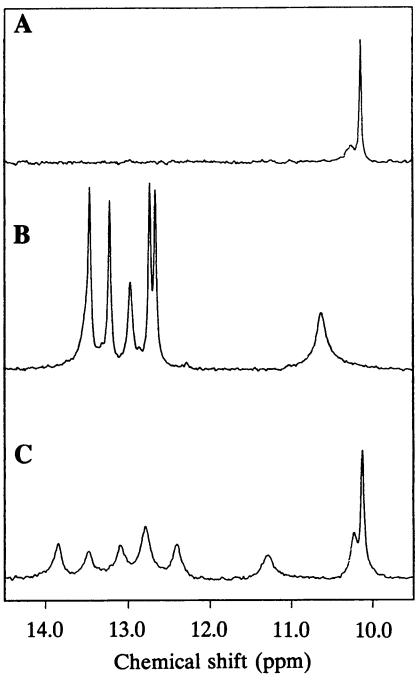

FIG. 6. NMR spectra. Downfield region of the ^1H NMR spectra of Nun protein (spectrum A), free *nutLboxB* RNA 16-mer (spectrum B), and a 1:1 complex of *boxB* RNA 16-mer with Nun protein (spectrum C). In spectra A and C, the $H^{\varepsilon 1}$ protons of Trp-33 and Trp-108 resonate at 10.2 ppm and 10.1 ppm, respectively. In spectra B and C, hydrogen-bonded imino protons of G and U bases resonate between 10 ppm and 14 ppm.

DISCUSSION

In this paper we have shown that Nun directly binds to the *boxB* stem–loop sequence of the λ *nut* RNA. Neither the *boxA* sequence of *nut* nor the host factors that participate in Nun transcription termination are required for this reaction. The K_d of the Nun–*boxB* RNA complex is estimated as 47.5 nM, about twice that of the λ N complex. The *boxB* loop nucleotide G in position 1 is critical for Nun binding, but most other loop nucleotides also contribute to the Nun–RNA interaction. RNase footprint experiments indicate that Nun and N protect the same loop and stem nucleotides of *boxB* RNA (ref. 11 and Fig. 3). This finding is supported by the observation that the two proteins compete for binding in solution.

The correlation between Nun binding *in vitro* and Nun termination *in vivo* is generally good. Thus, all base substitutions in *boxB* loop position 1 abolish both Nun binding *in vitro* and Nun termination *in vivo* (12). The *boxB* sequences of *nutR* and *nutL* differ in loop position 4 (A and G, respectively); the two *boxB* elements support Nun termination *in vivo* and bind Nun equally well *in vitro*. We note, however, that the 3C mutant binds weakly to Nun but does not inhibit Nun *in vivo* (17). The Nus factors, in addition to enhancing Nun activity, partially suppress certain *boxB* point mutations *in vitro* (15). The Nus factors might also suppress the 3C mutation *in vivo*.

Although loop mutants defective for N binding were in all cases defective in supporting N antitermination activity, the converse was not true. Some loop mutant RNAs bound N but did not support antitermination *in vitro* or *in vivo* (11). We

tested one such mutant, 4C, which also binds Nun efficiently, for Nun-dependent transcriptional arrest *in vitro*, using the assay system of Hung and Gottesman (15). As a control, we tested the 5C mutant, which is partially defective in Nun binding (Fig. 2). As expected, the 5C mutation reduced Nun-mediated transcription arrest. The 4C mutation, however, did not inhibit Nun activity in either the presence or the absence of the four Nus factors (data not shown). The 1U *boxB* mutation, which abolishes Nun binding, was shown previously to inhibit Nun-dependent transcription arrest in a minimal transcription system containing Nun and RNAP as the only proteins (15). Therefore, unlike the situation with N, the ability of a *boxB* variant to bind Nun correlates with its ability to support transcription arrest *in vitro*.

Nun and N share an N-terminal arginine-rich motif (ARM) found in several other RNA-binding proteins (20, 21). This ARM region has been shown by domain-swap experiments to determine the RNA target specificities of the various lambdoid phage N proteins, suggesting that the arginines make direct contact with the phage RNA (20). Critical residues in the ARM region of λ N that affect antitermination efficiency *in vivo* have been identified by extensive mutagenesis of the N protein (ref. 22 and Table 2). Additional evidence is presented here that indicates that the ARM region in Nun plays a role in RNA binding. First, NMR spectroscopy suggests that RNA binding changes the resonance of the Trp-33 residues that resides within the ARM region (Fig. 6). Second, RNA binding protects portions of Nun in the ARM region from digestion by trypsin (Fig. 4). Finally, the participation of the ARM region in *boxB* binding is indicated by *in vivo* studies of dominant negative N mutants and *in vitro* RNA-binding experiments with synthetic peptides (D. Lazinski, J. DeVito, S.C., and A.D., unpublished results). The ARM regions of Nun, λ N, and phage 22 N are aligned in Table 2. Of the known eight positions important for λ N function (22), Nun contains four identical residues and three "permitted" substitutions (substitutions shown to allow N function; ref. 22). Although it is tempting to explain the identical *boxB*-binding properties of Nun and N by this close similarity, phage 22 N is more homologous than Nun to λ N—with five identical residues and two permitted substitutions—and yet recognizes a distinct P22 *boxB* and is inactive on a λ *boxB* template (20).

Lazinski *et al.* (20) showed that the RNA-binding domain of λ N includes residues C-terminal to the ARM domain. Both those authors and Franklin (22) assert that the ARM domain is not the sole determinant of *boxB* binding specificity. Unfortunately, this notion does little to explain the similar, if not identical, binding specificities of Nun and N, since the two proteins have no discernible sequence homology other than within this domain. The mechanisms by which Nun and N bind RNA with such similar properties thus remain obscure.

Studies of Nun/N chimeras and of dominant negative truncated N mutants suggest that the C-terminal regions of the two proteins may interact in a specific way with RNAP and host factors to promote transcription termination or antitermination, respectively (K. Henthorn and D. Friedman, personal communication; J. DeVito, S.C., and A.D., unpublished results). For Nun termination, *boxB* may serve to tether Nun to the nascent transcript, increasing the local concentration of Nun in the vicinity of the transcribing RNAP. Trypsin protection assays suggest that *boxB* RNA also may conformationally "activate" the Nun protein.

Table 2. Comparison of λ N, HK022 Nun, and P22 N proteins

Protein	Residues	Sequence
λ N	3–17	**AQ**t**RRR**e**RR**aekqa**Q**
Nun	24–38	SRd**RRR**i**AR**wekri**A**
P22 N	15–29	**A**Kt**RR**He**RR**rklai*E*

The ARM regions of λ N, Nun, and P22 N proteins are aligned according to ref. 23. Residues in the ARM region known to be important for the antitermination activity of λ N *in vivo* (22) are shown in uppercase bold type. Permitted amino acid substitutions are in uppercase regular type, and substitutions with an unknown phenotype are in uppercase italic type. Residues shown in lowercase type are not believed to play an important role in N function. Residue numbers are shown in parentheses.

NMR spectroscopy reveals several interesting features of the Nun–*boxB* RNA complex. The change in resonance linewidth for Trp-33 $H^{\varepsilon 1}$ suggests that the environment of Trp-33, located in the ARM region, is more structured in the complex than in the free protein. This result is congruent with the trypsin assays. The altered resonance frequencies of the imino protons in the complex are a consequence of local interactions between *boxB* RNA and Nun. The notable broadening of the RNA imino resonances induced by Nun indicates that the RNA protons are in exchange on the intermediate chemical-shift (approximately millisecond) time scale. Broadening does not result from enhanced rates of solvent exchange of the imino protons in the complex, since exchange broadening is also observed for nonexchangeable ribose protons (data not shown). Exchange between free and bound RNA is slow on the chemical-shift time scale and does not explain the increased linewidths in the complex, because separate resonances for free and complexed *boxB* RNA are observed during the NMR titration. Thus, the broadening of the *boxB* RNA resonances may result from conformational changes, representing multiple bound forms of *boxB* RNA, within the RNA–protein complex. Additional NMR spectroscopic experiments will provide more direct information about structural changes upon complex formation.

We thank David Lazinski for the *nut21* clone, William Whalen for N protein, and David Friedman for communication of unpublished findings. This work was supported by National Institutes of Health Grants GM28946 (to A.D.) and GM37219 (to M.E.G.); National Science Foundation Grant MCB-9419049, an American Cancer Society Junior Faculty Research Award, and an Irma T. Hirschl Career Scientist Award (to A.P.); and National Institutes of Health Training Grant 2T32-EYO7105 (to A.S.).

1. Roberts, J. (1992) in *Transcriptional Regulation*, eds. McKnight, S. and Yamamoto, K. (Cold Spring Harbor Lab. Press, Plainview, NY), pp. 389–406.
2. Das, A. (1992) *J. Bacteriol.* **174,** 6711–6716.
3. Das, A. (1993) *Annu. Rev. Biochem.* **62,** 893–930.
4. Friedman, D. I. (1992) *Curr. Opin. Genet. Dev.* **2,** 727–738.
5. Greenblatt, J., Nodwell, J. R. & Mason, S. W. (1993) *Nature (London)* **364,** 401–406.
6. Olson, R. R., Flamm, E. L. & Friedman, D. I. (1983) *Cell* **31,** 61–70.
7. Barik, S., Ghosh, B., Whalen, W., Lazinski, D. & Das, A. (1987) *Cell* **50,** 885–899.
8. Horwitz, R. J., Li, J. & Greenblatt, J. (1987) *Cell* **51,** 631–641.
9. Whalen, W. & Das, A. (1990) *New Biol.* **2,** 975–991.
10. Nodwell, J. R. & Greenblatt, J. (1993) *Cell* **72,** 261–268.
11. Chattopadhyay, S., Garcia-Mena, J., DeVito, J., Wolska, K. & Das, A. (1995) *Proc. Natl. Acad. Sci. USA* **92,** 4061–4065.
12. Robert, L., Sloan, S. B., Weisberg, R. A., Gottesman, M. E., Robledo, E. & Harbrecht, D. (1987) *Cell* **51,** 483–492.
13. Robledo, R., Gottesman, M. E. & Weisberg, R. A. (1990) *J. Mol. Biol.* **212,** 635–643.
14. Sloan, S. B. & Weisberg, R. A. (1993) *Proc. Natl. Acad. Sci. USA* **90,** 9842–9846.
15. Hung, S. C. & Gottesman, M. E. (1995) *J. Mol. Biol.* **247,** 428–442.
16. Gottesman, M. E. & Weisberg, R. A. (1995) in *Seminars in Virology*, eds. Rothman-Denes, L. B. & Weisberg, R. A. (Academic, London), Vol. 6, pp. 35–42.
17. Baron, J. & Weisberg, R. A. (1992) *J. Bacteriol.* **174,** 1983–1989.
18. Robledo, R., Atkinson, B. L. & Gottesman, M. E. (1991) *J. Mol. Biol.* **220,** 613–619.
19. Milligan, J. F., Groebe, D. R., Witherall, G. W. & Uhlenbeck, O. C. (1987) *Nucleic Acids Res.* **15,** 8783–8788.
20. Lazinski, D., Grzadzielska, E. & Das, A. (1989) *Cell* **57,** 207–218.
21. Burd, C. G. & Dreyfuss, G. (1994) *Science* **265,** 615–621.
22. Franklin, N. C. (1993) *J. Mol. Biol.* **231,** 343–360.
23. Oberto, J., Weisberg, R. A. & Gottesman, M. E. (1989) *J. Mol. Biol.* **207,** 675–693.